Research Square

Preprints are preliminary reports that have not undergone peer review.
They should not be considered conclusive, used to inform clinical practice,
or referenced by the media as validated information.

Thermodynamic and structural properties of the thin atmosphere of a white dwarf

Riccardo Fantoni

rfantoni3@gmail.com

University of Trieste

Research Article

Keywords: White dwarf, Jellium, Path Integral, Monte Carlo, General Relativity, Thin surface layer, Thermodynamics, Structure

Posted Date: October 22nd, 2026

DOI: https://doi.org/10.21203/rs.3.rs-11267930/v1

License: This work is licensed under a Creative Commons Attribution 4.0 International License.
Read Full License

Additional Declarations: No competing interests reported.

Thermodynamic and structural properties of the thin atmosphere of a white dwarf

Riccardo Fantoni*
Università di Trieste, Dipartimento di Fisica, strada Costiera 11, 34151 Grignano (Trieste), Italy
(Dated: October 5, 2026)

We determine thermodynamic and structural properties of the Coulomb plasma (jellium) in the thin atmosphere of a white dwarf using the path integral Monte Carlo method within a general relativity description of the star.

Keywords: White dwarf;Jellium;Path Integral;Monte Carlo;General Relativity;Thin surface layer;Thermodynamics;Structure

CONTENTS

I. Introduction 1

II. Matter density matrix and the PIMC method 3

III. PIMC in a spatial foil of Schwarzschild metric 6

IV. PIMC Simulation on subatomic patch of the star atmosphere 8
A. Effect of the neutralizing background 9
B. The black hole limit 9

V. Numerical results 10

VI. Conclusions 12

Author declarations 13
Conflicts of interest 13
Data availability 13
Funding 13

References 13

I. INTRODUCTION

White dwarfs [1] are the dense remnants of stars, composed mainly of carbon and oxygen nuclei, which contain electrons, protons and neutrons and are supported against collapse induced by gravity by the electron degeneracy pressure due to Pauli exclusion principle. They remain white dwarfs till gravity overcomes electron degeneracy pressure, crushing electrons into protons to form neutrons through β^+ decay.

Therefore the simplest model for the interior of a white dwarf is that of *Jellium*. This is a system of pointwise electrons immersed in a uniform neutralizing background. The density of the electron gas is so high that the Fermi temperature is much higher than the temperature of the star and the electron gas can be considered degenerate. Chandrasekar [2–5] model of a white dwarf equilibrium structure didn't take into account the effects of general relativity. First Tolman [6], and later Oppenheimer and Volkoff [7] proposed a way to treat the hydrodynamic equations for the equilibrium and stability of a star within the framework of general relativity.

In order to make some progress towards a more realistic equation of state it is necessary to drop the assumptions of an ideal and perfect electron gas. This has been accomplished with various mean field theories. Since for a white dwarf the Wigner-Seitz radius is small, $0.0003 < r_s < 0.01$ the corrections due to the Coulomb interaction will be small. The main effect of the electrostatic corrections is to give smaller radii and larger central densities compared with Chandrasekhar models of the same mass. As described in §2.4 of the book [1] a first electrostatic correction arises because the positive charges are not uniformly distributed in the gas but are concentrated in individual nuclei. A

* riccardo.fantoni@scuola.istruzione.it

more accurate equation of state is needed for the strongly correlated plasma at high temperature and high density in the classical regime or at low temperature and low density in the quantum regime. Taking linearly into account charge screening in the electron-ion plasma a better approximation can be obtained from the Debye-Hückel theory in the classical regime or the Thomas-Fermi (and Thomas-Fermi-Dirac or Hartree-Fock) theory in the quantum regime. An even more accurate but non linear theory of screening is offered by Vlasov theory in the classical regime or Lindhard (also known as random phase approximation) theory in the quantum regime [8]. Apart from these mean field theories, perturbative [9] or integral equation [10] approaches are also available.

More progress towards an exact solution of the model of the plasma is otherwise possible employing numerical computer experiments like path integral Monte Carlo [11] at finite non zero temperature or diffusion Monte Carlo [12, 13] at zero temperature. In order to take into account the effects of general relativity in the equation of state to be used within the Tolman-Oppenheimer-Volkoff equilibrium it is then necessary to solve a path integral Monte Carlo experiment for an electron or an electron-ion plasma within general relativity.

We can then proceed following two distinct routes, either we treat the quantum particles as living in a classical (non-quantum) spacetime or classical (non-quantum) particles living in a quantum spacetime [14]. In this work we propose to use the former route as we will *discuss* in Sec. II.

This welding of *causality*, inherent in general relativity, and *casuality*, inherent in the Monte Carlo method, is expected to offer an operative approach to the problem of (quantum) statistical gravity of many body liquids [14–19]. The melt between the superposition principle of quantum physics and the non linearity of general relativity is still under construction.

The luminosity of a white dwarf is due to a thin radiating layer on the star surface (see chapter 4 of the book [1]). The mechanism of a white dwarf cooling is the primary bridge between our theoretical description of the star and observational data which rely on essentially two aspects: luminosity observations and time scale of the observed cooling.

Purpose of this work is to determine the thermodynamic and structural properties of the electron plasma in this thin atmosphere using the path integral Monte Carlo (PIMC) method [11] at low non zero temperature. In order to take into account the effects of general relativity we will use the $3+1$ foliation of Arnowitt, Deser, and Misner (ADM) [20] to build a matter density matrix from the stress-energy tensor through a path integral where on each imaginary timeslice one selects a constant time foil [21]. This amounts to treat the quantum Coulomb plasma in the classical Schwarzschild spatial metric in a patch of subatomic dimensions at the radius $\mathscr{R}$ of the star of mass $\mathscr{M}$. In weak gravity the determinant ${}^3g$ of the spatial components of the metric tensor is such that $-\ln\sqrt{{}^3g} \approx -\ln(r^2|\cos\theta|) - \Phi/c^2$ with $\Phi = GM/r$ the Newtonian *gravitational potential*. We propose to use a *geometrical potential* acting on each electron $w = -\hbar[\ln\sqrt{{}^3g}]/\tau$ with τ the imaginary time step used in the discretization of the path integral. On the other hand we will neglect the physical gravitational potential of the gravitating electrons that should otherwise be included through the introduction of the Tolman-Ehrenfest temperature [22, 23].

The problem of the plasma on the surface of a sphere, has already been treated in Refs. [19, 24, 25]. Here the two dimensional curved surface of the sphere is substituted by the three dimensional spatial Schwarzschild foil of the white dwarf.

We may assume that the electrons dispersion relation is the one of non relativistic particles $\epsilon(p) = p^2/2m$. This is reasonable since the density of the electron-proton plasma [1] in the thin surface layer is $\rho_l \approx 10^3 \mathrm{g/cm}^3$ (see section 4.1 of the book [1]) much lower than the central densities, corresponding to $r_s \approx 0.2$. Therefore $p_F^2/m^2c^2 \approx 0.01$ where m is the electron mass and $p_F = h(3n/4\pi)^{1/3}$ is the polarized electrons Fermi momentum. The temperature of the surface layer falls in the range $10^6\mathrm{K} \lesssim T \lesssim 10^7\mathrm{K}$. We will consider a white dwarf with a radius $\mathscr{R} \approx 700\mathrm{Km}$ and a mass $\mathscr{M} \approx 2 \times 10^{30}\mathrm{Kg}$, so the Schwarzschild radius is about $R_{\mathrm{Sc}} \approx 3\mathrm{Km}$.

We will determine the effect of temperature, quantum statistics, gravity, and of imposing charge neutrality on the weakly correlated electron plasma in the quantum regime. The plasma we are confronting with move from the lower left corner of the phase diagram of figure 1 of Ref. [26] for the Euclidean jellium.

The paper is organized as follows: In Sec. II we discuss the matter density matrix approach; in Sec. III we define the PIMC used in the simulations; in Sec. IV we specify the characteristics of the patch; in Sec. V we present our numerical results; Sec. VI is for conclusive remarks.

---

[1] Assuming that the white dwarf is made up of a completely ionized plasma then we may write $\rho = \mu_e m_u n$ with n the electrons number density, m_u the atomic mass unit, and $\mu_e = A/Z$ with Z the atomic number and A the mass number, so that for example for a ^{4}He or a ^{12}C white dwarf $\mu_e = 2$ and for a ^{56}Fe white dwarf $\mu_e = 56/26 \approx 2.134$.

II. MATTER DENSITY MATRIX AND THE PIMC METHOD

In Ref. [14] we discussed a thermal equivalence principle that should hold when dealing with a statistical physics theory of a many body fluid within the framework of general relativity: Einstein field equations $G_{\alpha\beta} = (G8\pi/c^4)T_{\alpha\beta}$ suggest that the statistical properties *of spacetime*, determined by the Einstein-Hilbert action [15–17], and the statistical properties *of matter* moving in it, determined solely by the right hand side of Einstein equations, the stress energy tensor, should be equivalent, one should be the shadow of the other. In particular when looking at the right hand side we may assume for the density matrix of the many (scalar) particle system the following expression

$$\hat{\rho} = \exp\left(-\int_{\partial\Omega} \hat{T}^{\alpha\beta}\,\beta_\alpha\, dS_\beta\right), \tag{2.1}$$

that holds in quantum statistical mechanics within special relativity [27]. In Eq. (2.1) we use Einstein convention to tacitly assume a sum over repeated indexes. We will assume that this expression continues to hold also within general relativity. We will use a hat to denote the corresponding operator, $\partial\Omega$ to denote an arbitrary spacelike hypersurface bounding the four dimensional region Ω of the curved spacetime occupied by the N particles, and β^α a vector such that $\sqrt{\beta_\alpha\beta^\alpha} = 1/k_BT$ with k_B Boltzmann constant and T the absolute temperature.

Within Arnowitt, Deser, and Misner (ADM) $3+1$ foliation of space and imaginary time [17] we can evaluate the integral at the exponent of Eq. (2.1) choosing a hypersurface orthogonal to the time component so that $dS_0 = \prod_{\mu=1}^N \sqrt{{}^3g(\boldsymbol{r}_\mu)}\, d\boldsymbol{r}_\mu$ where ${}^3g = \det\{g_{ij}\} > 0$ with g_{ij} the metric on the spatial components and $\boldsymbol{r}_\mu$ the *shifted* spatial positions of the μ particle, with $d\boldsymbol{r}_\mu = d\boldsymbol{x}_\mu + \boldsymbol{N}cdt_\mu$. Here $\vec{\boldsymbol{x}}_\mu = (t_\mu, \boldsymbol{x}_\mu)$ is the 4–vector event for particle μ and $\boldsymbol{N}$ is the *shift* in the ADM foliation

$$ds^2 = g_{\alpha\beta}dx^\alpha dx^\beta = L^2c^2dt^2 + g_{ij}(dx^i + N^i c\,dt)(dx^j + N^j c\,dt),$$

with

$$||g_{\alpha\beta}|| = \begin{pmatrix} L^2 + N^iN_i & N_i \\ N_i & g_{ij} \end{pmatrix}, \tag{2.2}$$

where L is the *lapse* and N^i the ith spatial component of the shift (see Eq. (4) in [17]). By Birkhoff theorem the vacuum solution of Einstein field equations outside a mass $\mathscr{M}$ is the one of Schwarzschild for which the shifts are zero $L^2 = (1 - R_{\rm Sc}/r)$ and $g_{rr} = (1 - R_{\rm Sc}/r)^{-1}, g_{\theta\theta} = r^2, g_{\varphi\varphi} = r^2\cos^2\theta$ with $R_{\rm Sc} = 2G\mathscr{M}/c^2$ the Schwarzschild radius with $\mathscr{M}$ the mass of the star inside the spherical shell, by Birkhoff theorem. So that ${}^3g = (1 - R_{\rm Sc}/r)^{-1}r^4\cos^2\theta > 0$ with $r \gg R_{\rm Sc}$. Where for a typical white dwarf $\mathscr{R}/R_{\rm Sc} \sim 10^3$. We will generally use a Greek index to denote one of the 4 spacetime components and a Roman index to denote one of the 3 spatial components. A bold face symbol denotes its status as a three dimensional vector.

We may then introduce

$$\tilde{g}_{ij}(R) \;=\; g_{i_1j_1}(\boldsymbol{r}_1) \otimes \ldots \otimes g_{i_Nj_N}(\boldsymbol{r}_N), \tag{2.3}$$

$$\tilde{g}(R) \;=\; \prod_{\mu=1}^N {}^3g(\boldsymbol{r}_\mu), \tag{2.4}$$

where $||\tilde{g}_{ij}||$ is a matrix made of N diagonal blocks $||g_{i_\mu j_\mu}||$ with $\mu = 1, 2, \ldots, N$ and $R = \{\boldsymbol{r}_1, \ldots, \boldsymbol{r}_N\}$ the shifted spatial positions of the N particles.

By the definition of the stress-energy tensor

$$\int \hat{T}^{00}\, dS_0 = \hat{\mathscr{H}}_N, \tag{2.5}$$

where $\hat{\mathscr{H}}_N$ is the Hamiltonian operator of the N particles *without* their gravitational potential energy. For a fluid invariant under translations and rotations [2] this is the only stress-energy tensor component entering the density matrix in Eq. (2.1) [27].

We then reach the following expression

$$\hat{\rho} = \exp\left(-\beta_0\hat{\mathscr{H}}_N\right), \tag{2.6}$$

[2] Here we mean invariant under the relative killing vector or isometry, i.e. a transformation that leaves the metric tensor unchanged.

satisfying to Bloch equation

$$\frac{\partial\hat{\rho}}{\partial\beta_0} = -\hat{\mathscr{H}}_N\hat{\rho}, \tag{2.7}$$

$$\hat{\rho}(0) = \mathbb{1}, \tag{2.8}$$

where $\mathbb{1}$ the identity matrix. Here we choose $\beta_0\sqrt{\tilde{g}^{00}} = 1/k_BT$ or $\beta_0(R) = 1/k_B\tilde{T}(R) = \sqrt{\tilde{g}_{00}(R)}/k_BT$ with $\tilde{T}(R) = T/\sqrt{\tilde{g}_{00}(R)}$ the Tolman-Ehrenfest temperature [22, 23]. This procedure is quite unorthodox since it assumes already a position representation for the temperature but as we will see later it correctly *includes* the gravitational potential energy. On the other hand it neglects the self-gravitation of the particles. In order to include them one should solve a self consistent field problem. Instead of treating the spacetime metric as a fixed background, the gas particles themselves act as a source of stress-energy that alters the spacetime curvature [6, 7, 28].

The coordinates, R, representation of the density matrix (2.6) can then be expanded into a path integral [11]

$$\rho(R,R';\beta_0) = e^{-\mathscr{S}_N/\hbar} = \int \rho(R,R_1;\tau)\cdots\rho(R_{M-1},R';\tau)\prod_{k=1}^{M-1} d^{3N}R_k, \tag{2.9}$$

where $\mathscr{S}_N = \int_0^{\hbar\beta_0} H_N\,dt$ is the action, $\tau(R) = \hbar\beta_0(R)/M$ is a small imaginary *timestep*, and the *primitive approximation* [11] to the high temperature, $M \gg 1$, density matrix

$$\rho(R,R';\tau) \propto \sqrt{\tilde{g}(R)}\exp-\frac{1}{\hbar}\left[\sum_{\mu=1}^{N} g_{ij}(\boldsymbol{r}_\mu)(r^i_\mu - r'^i_\mu)(r^j_\mu - r'^j_\mu)/4\lambda\tau(R) + \tau(R)\,V_N(R)\right], \tag{2.10}$$

where $H_N = K_N + V_N$ is the classical Hamiltonian with V_N the potential energy due to the N particles mutual interactions and we assumed *non relativistic* $k_BT \ll mc^2$ [14] particles with a kinetic energy in a local Lorentz frame $-\lambda\sum_{\mu=1}^{N}\nabla^2_\mu$ with $\lambda = \hbar^2/2m$. Fully relativistic particles with a dispersion relation in a local Lorentz frame, $\epsilon(\boldsymbol{p}) = \sqrt{(\boldsymbol{p}c)^2 + (mc^2)^2}$ with $\boldsymbol{p} = -i\hbar\nabla$, are *non-local* even in the Lorentz frame since the Taylor expansion of ϵ in $\boldsymbol{p}$ has ever increasing powers of $\boldsymbol{p}$. In order to restore locality is therefore necessary to imagine for each particle the presence of its *antiparticle* [29] with negative energy $\bar{\epsilon}(\boldsymbol{p}) = -\sqrt{(\boldsymbol{p}c)^2 + (mc^2)^2}$. In the action in Eq. (2.10) we recover the classical kinetic energy $\sum_{\mu=1}^{N}\frac{1}{2}m(ds_\mu/\tau)^2$ where ds_μ is the proper distance for the dislpacement of particle μ on the apatial foil in a Tolman-Ehrenfest timestep τ. Attempts have also been tried in the fully relativistic case like the use of Fock 'fifth parameter' by Feynmann which nonetheless, despite its intuitive and creative nature, brings about some new physical interpretations not yet tested experimentally like the Hawking black hole evaporation as described in chapter 25 of the book [30].

In Eq. (2.9), at each timeslice $t_k = k\tau$, for $k = 1, 2, \ldots, M-1$, we consider the section of spacetime at constant imaginary time and construct the high temperature density matrix on that spatial foil. Eq. (2.10) reduces to the usual expression in Euclidean space [11]. It has been found that one may need corrections due to the curvature of space and to the van Vleck determinant [30, 31]. The curvature of a spatial foil of the Schwarzschild metric is zero. In fact, contracting Einstein field equations in vacuum implies a vanishing scalar curvature, the trace of Ricci tensor. Then Einstein field equations in vacuum reduce to the vanishing of the Ricci tensor. Therefore also the scalar curvature of a spatial foil, at constant time, of Schwarzschild metric must vanish. On the other hand the van Vleck determinant in the high temperature limit reduces to 1.

The most general case requires taking care also of the self gravitation of the electrons. One then would like to use self consistently the metric g_{ij} obtained solving Einstein field equations for each particles configuration at the given timeslice generated by the Metropolis random walk [11, 32, 33].

In the high temperature regime one recovers the *classical statistical mechanics* For $M = 1$ and $R \approx R'$

$$\rho(R,R';\tau) \propto \sqrt{\tilde{g}(R)}\exp-\frac{1}{\hbar}\left[\tau(R)\,H_N\right], \tag{2.11}$$

where $\tau(R) = \hbar\beta_0(R)$.

Up to here we treated the particles as distinguishable. On the other hand the properties of a quantum many body fluid depend on the kind of quantum statistics, either Bose-Einstein or Fermi-Dirac, obeyed by its identical particles.

Therefore we are rather interested in [11, 34] [3]

$$\rho_{\rm B,F}(R,R';\beta_0) \;=\; \frac{1}{N!}\sum_{\mathscr{P}} {\rm sgn}(\mathscr{P})\rho(\mathscr{P}R,R';\beta_0), \tag{2.12}$$

$${\rm sgn}(\mathscr{P}) \;=\; (\pm 1)^{\sum_{\nu=1}^{N}(\nu-1)C_\nu}, \tag{2.13}$$

where $\mathscr{P}$ is any permutation of the N particles such that $\mathscr{P}R = (\boldsymbol{r}_{\mathscr{P}1}, \boldsymbol{r}_{\mathscr{P}2}, \dots, \boldsymbol{r}_{\mathscr{P}N})$, with sign ${\rm sgn}(\mathscr{P})$. For bosons ${\rm sgn}(\mathscr{P}) = +1$. For fermions an even (odd) permutation has ${\rm sgn}(\mathscr{P}) = +1(-1)$ and an even (odd) number of exchanges of a pair of particles. Any permutations can be broken into cycles $\mathscr{P} = \{C_\nu\}$ where C_ν is the number of cycles of length ν in $\mathscr{P}$. We may then introduce a deBroglie thermal wavelength

$$\Lambda(R) = \sqrt{2\lambda\beta_0(R)}, \tag{2.14}$$

dependent on the point in the $3N$ manifold. When the size, $\Lambda(R)$, of the many body path $R_1, R_2, \dots R_M$ equals the interparticle spacing, $n^{-1/3}$ with n the proper particle number density, the permutations will have an effect on the measure of diagonal observables. This determines a degeneracy temperature

$$T_D = \frac{2\lambda n^{2/3}}{k_B}. \tag{2.15}$$

We may then introduce an adimensional parameter $\Theta = T/T_D$ such that for $\Theta \ll 1$ quantum statistics will be very important.

This expression correctly reduces to the density matrix of the classical, $\Theta \gg 1$, system of non relativistic, $p/mc \ll 1$, particles in weak gravity, $\Phi/c^2 \ll 1$ with $\Phi(r) = G\mathscr{M}/r$ with $\mathscr{M}$ the mass of the star. In fact $\sqrt{\tilde{g}_{00}(R)} \approx \prod_{\mu=1}^{N}[1 - \Phi(r_\mu)] \approx 1 - \sum_{\mu=1}^{N}\Phi(r_\mu)$. So that

$$\frac{\tau(R)\,H_N}{\hbar} = \frac{1}{k_B T M}\left(\sum_{\mu=1}^{N}\frac{p_\mu^2}{2m} - mc^2\sum_{\mu=1}^{N}\frac{G\mathscr{M}}{c^2 r_\mu} + V_N(R) + \dots\right), \tag{2.16}$$

where we neglected terms of second order in the small quantities p/mc and $GM/c^2 r$.

We have previously proposed [35] to consider the $\sqrt{\tilde{g}(R)}$ factors as an external geometrical potential

$$W_N(R) = -\ln\left[\sqrt{\tilde{g}(R)}\right]\hbar/\tau(R) + \dots, \tag{2.17}$$

where the dots stand for additional corrections due to the space curvature and the van Vleck determinant [30, 31]. These contributions can more easily be taken into account by a change of coordinates which transform the Laplace-Beltrami operator into the flat Laplacian, solving Bloch equation (2.7) in the new coordinates and then reverting to the original ones [36].

The classical limit (2.11) has been used in various spatial dimensions to describe the properties of Coulomb systems. These offer some exact analytic solutions in one dimension [37, 38], in two dimensions [39], and at a special value of the coupling constant in two dimensions on various surfaces: The plane [40], the cylinder [41], the sphere [42], the pseudosphere [43], the Flamm paraboloid [44, 45]. [4]

On the other hand, the path integral (2.9) with the primitive approximation (2.10) has been treated for example in Refs. [30, 31] and applied in various geometries to various physical systems. For the example of the sphere treated with the Monte Carlo method [33] see Refs. [19, 24, 25].

In order to extract the statistical mechanics properties of a many (scalar) particle fluid within general relativity, we chose to work on the right hand side of Einstein field equations, building a density matrix from the stress-energy tensor through a path integral where on each imaginary timeslice one selects a constant time foil of the $3+1$ ADM spacetime foliation.

This Matter Density Matrix (MaDM) should follow as a shadow the equivalent Metric Density Matrix (MeDM) constructed from the Einstein-Hilbert action, which gives a statistical mechanics of spacetime [17]. It is our impression

---

[3] One can antisymmetrize respect to the first, the second, or both the arguments of the distinguishable density matrix. We here choose the first case.

[4] In $d+1$ spacetime with $d \leq 2$ the Weyl conformal tensor vanishes and the Riemann tensor is completely determined by its trace, the Ricci tensor. Contracting Einstein field equations in vacuum implies a vanishing scalar curvature, the trace of Ricci tensor. Then Einstein field equations in vacuum reduce to the vanishing of the Ricci tensor and consequently to the vanishing of the whole Riemann tensor. It is only in $d > 2$ that general relativity looks like a theory of the gravitational interaction. Nonetheless Flamm paraboloid is an interesting surface of non constant curvature where the Coulomb plasma still admits an exact analytic solution.

that among the two equivalent routes to statistical physics this last one offers a mathematically much more cumbersome approach [46]. Nonetheless the use of the Markov stochastic processes, inherent to the Metropolis algorithm [32], to measure a structural or thermodynamic observable of the many body fluid should make no distinction among the two routes. In fact the Metropolis algorithm is very simple and powerful; it can be used to sample essentially any probability distribution function regardless of analytic complexity in any number of dimensions.

In the rest of this work we will choose the Tolman-Ehrenfest temperature equal to the absolute temperature $\tilde{T}(R) = T$. As we discussed this amounts to neglect the gravitational potential energy for the interaction of the electrons with the star. We will also redefine the matter density matrix of Eq. (2.10) without the geometrical factor $\sqrt{\tilde{g}(R)}$ and include it as a measure of integration in the path integral expression of Eq. (2.9).

From now on we will use natural Planck units $c = G = \hbar = k_B = 1$ where c is the speed of light, $\hbar$ is the reduced Planck constant, G is the gravitational constant, and k_B is the Boltzmann constant.

III. PIMC IN A SPATIAL FOIL OF SCHWARZSCHILD METRIC

A many body system composed of N *distinguishable* particles of mass m with positions in $R = (\boldsymbol{r}_1, \boldsymbol{r}_2, \ldots, \boldsymbol{r}_N) = (\{\boldsymbol{r}_l\})$ where each position vector $\boldsymbol{r}_i = (r_l^1, r_l^2, r_l^3) = (\{r_l^j\}) = (\{r^{j_l}\})$ in 3 dimensions. On a foil of Schwarzschild solution (2.2) with spatial metric tensor $g_{ij}(\boldsymbol{r})$, the geodesic distance between two infinitesimally close points R and R' is $d\tilde{s}^2(R, R') = \sum_{l=1}^{N} ds^2(\boldsymbol{r}_l, \boldsymbol{r}_l')$ where $ds^2(\boldsymbol{r}, \boldsymbol{r}') = g_{ij}(\boldsymbol{r})(\boldsymbol{r} - \boldsymbol{r}')^i(\boldsymbol{r} - \boldsymbol{r}')^j$.

The Laplace-Beltrami operator on the manifold of dimension $3N$ is

$$\Delta_R = \tilde{g}^{-1/2}\nabla_i(\tilde{g}^{1/2}\tilde{g}^{ij}\nabla_j), \tag{3.1}$$

where $\nabla = \nabla_R$, $\tilde{g}^{ij}$ is the inverse of $\tilde{g}_{ij}$, i.e. $\tilde{g}_{ij}\tilde{g}^{jk} = \delta_i{}^k$ the Kronecker delta.

The Hamiltonian $\mathscr{H}$ of the N non relativistic particles will be

$$\mathscr{H} = -\lambda\Delta_R + V(R), \tag{3.2}$$

where $\lambda = 1/2m$ and $V(R)$ is the *Coulomb potential* energy of the system, that we here assume only a function of the particles positions and bounded from below.

The density matrix ρ of the system obeys to Bloch equation (2.7) where we now drop the hat on the operators and the subscript N. The position representation of the density matrix is then obtained from $\rho(R, R'; t) = \langle R|\rho(t)|R'\rangle$ with $\langle R|R'\rangle = \delta(R - R')/\sqrt{\tilde{g}(R)}$ where δ is a $3N$ dimensional Dirac delta function. In the small imaginary time τ limit the position representation of the density matrix is [19]

$$\rho(R, R'; \tau) \propto \tilde{g}(R)^{-1/4}\sqrt{\mathscr{D}(R, R'; \tau)}\,\tilde{g}(R')^{-1/4}e^{\lambda\tau\mathscr{R}(R)/6}e^{-\mathscr{S}(R,R';\tau)}, \tag{3.3}$$

where $\mathscr{R} = 0$ is the scalar curvature of the Schwarzschild spatial foil [5], $\mathscr{S}$ the action, and $\mathscr{D}$ the van Vleck's determinant [30, 47]

$$\mathscr{D}_{\mu\nu} = -\nabla_\mu\nabla'_\nu\mathscr{S}(R, R'; \tau), \tag{3.4}$$

$$\det||\mathscr{D}_{\mu\nu}|| = \mathscr{D}(R, R'; \tau), \tag{3.5}$$

where $\nabla = \nabla_R$ and $\nabla' = \nabla_{R'}$. This determinant is the Jacobian of the transformation from the initial conditions given by fixing the pair of momentum and coordinate of each particle to the boundary conditions given by specifying the pair of initial and final coordinates needed in the coordinate representation. The square root of the van Vleck determinant factor takes into account the density of paths among the minimum extremal region for the action (see Chapter 12 of Ref. [30]). The two factors $\tilde{g}^{-1/4}$ are needed in order to have for the density matrix a bidensity for which the boundary condition to Bloch equation is simply a Dirac delta function. In the small $\tau \to 0$ limit [6] $\tilde{g}(R)^{-1/4}\sqrt{D(R, R'; \tau)}\,\tilde{g}(R')^{-1/4} \to (1/2\lambda\tau)^N$.

For the *action* $\mathscr{S}$, the *kinetic-action* $\mathscr{K}$, and the *inter-action* $\mathscr{U}$ we have [7]

$$\mathscr{S}(R, R'; \tau) = \mathscr{K}(R, R'; \tau) + \mathscr{U}(R, R'; \tau), \tag{3.6}$$

$$\mathscr{K}(R, R'; \tau) = \frac{dN}{2}\ln(4\pi\lambda\tau) + \frac{d\tilde{s}^2(R, R')}{4\lambda\tau}. \tag{3.7}$$

---

[5] The factor depending on the curvature of the manifold is due to Bryce DeWitt [31]. For a space of constant curvature there is clearly no effect, as the term due to the curvature just leads to a constant multiplicative factor that has no influence on the measure of the various observables.

Contracting Einstein field equations in vacuum implies a vanishing scalar curvature, the trace of Ricci tensor. Then Einstein field equations in vacuum reduce to the vanishing of the Ricci tensor. Therefore also the scalar curvature of a spatial foil, at constant time of Schwarzschild metric must vanish.

[6] Remember that the metric tensor is covariantly constant.

[7] The expression for $\mathscr{K}$ is the one of Eq. (24.16) of Ref. [30] to lowest order in $R - R'$.

In particular the kinetic-action is responsible for a diffusion of the random walk with a single particle variance equal to $\sigma_{ij}^2(\boldsymbol{r}) = 2\lambda\tau/g_{ij}(\boldsymbol{r})$. The inter-action is defined as $\mathscr{U} = \mathscr{S} - \mathscr{K}$ and for potential energies bounded from below one can resort to the Trotter formula [48] to reach the *primitive approximation* [8]

$$\mathscr{U}(R, R'; \tau) = \tau[V(R) + V(R')]/2. \tag{3.8}$$

Given then an observable $\mathscr{O}$ we can determine its thermal average at an absolute temperature T from

$$\langle\mathscr{O}\rangle = g_s \mathrm{tr}\{\rho(\beta)\mathscr{O}\}/Z_N, \tag{3.9}$$

$$Z_N = g_s \mathrm{tr}\{\rho(\beta)\}, \tag{3.10}$$

where $\beta = 1/T$, $\mathrm{tr}\{\ldots\}$ is the trace over the spatial variables, Z_N the canonical partition function, $g_s = 2s+1$ is the spin degeneracy, and we assumed the Hamiltonian independent from spin. For *identical* bodies the spin-statistics theorem of quantum field theory, dictates that in spatial dimension bigger than two, particles with integer spin are bosons (obeying Bose-Einstein statistics, symmetric wavefunctions), while half-integer spin particles are fermions (obeying Fermi-Dirac statistics, antisymmetric wavefunctions). We will only consider polarized electrons that are fermions with $g_s = 1$.

The position representation of the density matrix at an imaginary time $t = \beta$ is obtained through a *path integral*

$$\rho(R, R'; \beta) = \langle R|\rho(\beta)|R'\rangle = \int \rho(R_0, R_1; \tau) \prod_{k=1}^{M-1} \left[\rho(R_k, R_{k+1}; \tau)\sqrt{\tilde{g}(R_k)}\, dR_k\right] \delta(R_0 - R)\delta(R_M - R')\, dR_0 dR_M, \tag{3.11}$$

where we have discretized the imaginary time β into M *timeslices* with a small *timestep* $\tau = \beta/M$. The volume element of integration, $\sqrt{\tilde{g}(R)}\, dR$, can be treated by introducing $W(R) = -[\ln\sqrt{\tilde{g}(R)}]/\tau$ as an effective *geometrical potential*. The many body path $R(t)$ is consequently discretized in M *beads* $R_k = (\{\boldsymbol{r}_{l,k}\}) = (\{r^j_{l,k}\})$ at each timeslice $k = 1, 2, \ldots, M$. We will also call *link* a pair of contiguous beads. Note that in order to measure an observable through Eq. (3.9) it is necessary to consider closed paths such that $R(t+\beta) = R(t)$, or rings on the foil.

For identical electrons, that satisfy to the Fermi-Dirac statistics, one needs to antisymmetrize the distinguishable density matrix (3.11) [34]. We will then use ρ_F of Eq. (2.12).

We will model the Coulomb plasma in the white dwarf atmosphere as an electron gas of N electrons, i.e. a jellium where initially we neglect the uniform neutralizing background [9]. The Coulomb potential energy is then

$$V(R) = \sum_{m<n} \phi(\boldsymbol{r}_m, \boldsymbol{r}_n), \tag{3.13}$$

with ϕ the Coulomb pair potential between a charge q_m at $\boldsymbol{r}_m$ and a charge q_n at $\boldsymbol{r}_n$. The exact analytical expression for ϕ is given by the Copson-Linet potential [49–51] [10]

$$\phi(\boldsymbol{r}_1, \boldsymbol{r}_2) = \frac{q_1 q_2}{r_1 r_2}\left[\frac{(r_1 - \mathscr{M})(r_2 - \mathscr{M}) - \mathscr{M}^2\cos\gamma_{12}}{\sqrt{(r_1-\mathscr{M})^2 + (r_2-\mathscr{M})^2 - 2(r_1-\mathscr{M})(r_2-\mathscr{M})\cos\gamma_{12} - \mathscr{M}^2\sin^2\gamma_{12}}} + \mathscr{M}\right], \tag{3.14}$$

where

$$\cos\gamma_{12} = \sin\theta_1\sin\theta_2 + \cos\theta_1\cos\theta_2\cos(\varphi_1 - \varphi_2), \tag{3.15}$$

and the Linet topological term $q_1 q_2 \mathscr{M}/r_1 r_2$ is an isotropic, long-range, mutual energy correction ensuring that the presence of the Schwarzschild singularity doesn't introduce unphysical net charge accumulation [11]. In our white dwarf scenario, in Planck units, $\mathscr{M} \sim 10^{38} \ll \mathscr{R} \sim 10^{40}$ and this term will be small. In the flat spacetime $\mathscr{M} \to 0$

$$\phi(\boldsymbol{r}_1, \boldsymbol{r}_2) \to \frac{q_1 q_2}{\sqrt{r_1^2 + r_2^2 - 2r_1 r_2\cos\gamma_{12}}}. \tag{3.17}$$

---

[8] See Ref. [11] for a numerical analysis of the accuracy of this approximation and for its possible refinements.

[9] In a jellium Eq. (3.13) should be substituted by

$$V(R) = \sum_m \phi_b(r_m) + \sum_{m<n}\phi(\boldsymbol{r}_m, \boldsymbol{r}_n), \tag{3.12}$$

with ϕ_b the potential energy due to the uniform proper charge density $\rho_b = -ne$ of the neutralizing background as described in Section IV A. Since ϕ_b is just a shallow harmonic pull at the center of the patch we will initially neglect it.

[10] Compare with the one on a Flamm paraboloid [44].

[11] Note that since the angular distances are extremely small, for example of the order of 10^{-17} in case A of Table I, we can use the following approximation

$$\phi(\boldsymbol{r}_1, \boldsymbol{r}_2) = \frac{q_1 q_2}{r_1 r_2}\left[\frac{(r_1 - \mathscr{M})(r_2 - \mathscr{M}) - \mathscr{M}^2}{\sqrt{(r_1 - r_2)^2 + 2(r_1-\mathscr{M})(r_2-\mathscr{M})(1-\cos\gamma_{12})}} + \mathscr{M}\right], \tag{3.16}$$

where we may expand $\cos\gamma - 1$ to first order in θ_i, φ_i. We are allowed to approximate the $cos\gamma_{12} \approx 1$ in the numerator since $\mathscr{M}\theta_0^2/\mathscr{R} \sim 10^{-36}$. We are also allowed to neglect the term $\mathscr{M}^2\sin^2\gamma_{12}/\mathscr{R}^2 \approx (\mathscr{M}\theta_0/\mathscr{R})^2 \sim 10^{-39}$. Note that on a computer in order to be able to calculate the difference $r_1 - r_2$ between two electrons of the patch we need quadruple precision since $\mathscr{R} \sim 10^{40}$ and $\delta \sim 10^{23}$ so we need at least 17 significant digits. Since we have wall boundary conditions on r and periodic boundary conditions on θ, φ, in order to fulfill the minimum image convention, given θ_1, φ_1 we will choose the image of θ_2, φ_2 which gives the minimum $1 - \cos\gamma_{12}$.

IV. PIMC SIMULATION ON SUBATOMIC PATCH OF THE STAR ATMOSPHERE

From exercise 4.1 of the book [1] follows that the depth of the thin radiating surface layer of a white dwarf is

$$\mathscr{D} \lesssim 10^{-2}\mathscr{R}, \tag{4.1}$$

where the typical radius of a white dwarf is $\mathscr{R} \approx 10^{-3}R_\odot - 10^{-2}R_\odot$.

In order to treat the problem of electrons constrained in a subatomic patch of a thin spherical shell of width $\delta \ll \mathscr{D}$ we imagine an infinite repulsive external potential at $r > \mathscr{R}$ and at $r < \mathscr{R} - \delta$ In the Monte Carlo we reject any move that brings an electron in these regions in oredr to simulate wall boundary conditions on r. On the other hand we will adopt periodic boundary conditions on θ and φ with periodicities θ_0 and φ_0 respectively. We will choose $\theta_0 = \varphi_0$. We want the radial extent of the patch comparable to the angular extent so we will choose $\delta \approx \mathscr{R}\theta_0$. In Fig. 1 we show a diagram illustrating the patch.

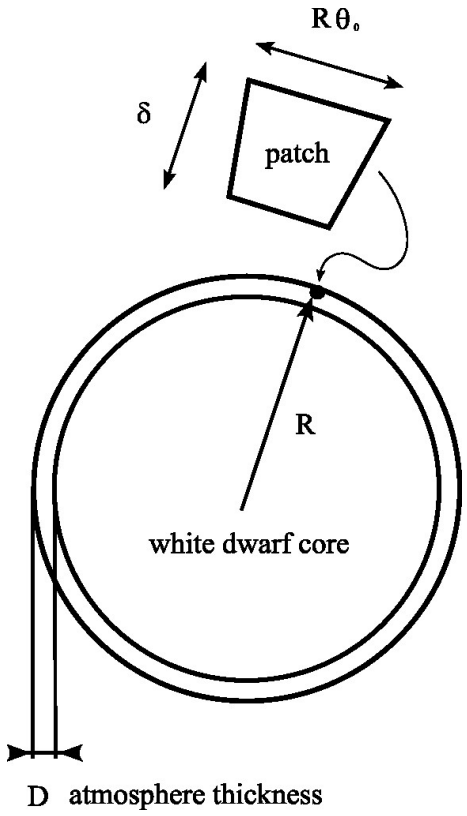


FIG. 1. Diagram illustrating the patch used in the simulations.

Of course this is a first brute approximation to a more realistic model including an 'osmosis' of electrons between the patch of the white dwarf atmosphere and the star interior. Using periodic boundary conditions on the spherical angles we model a thin spherical shell of radial width δ. Even if we will not worry about finite size errors which occur inevitably due to the choice of $\theta_0 \ll \pi/2$.

The Cartesian coordinates of a particle on the Schwarzschild spatial foil is

$$\begin{cases} x = r\cos\theta\cos\varphi \\ y = r\cos\theta\sin\varphi \\ z = r\sin\theta \end{cases} \tag{4.2}$$

where $r^1 = r \in [\mathscr{R} - \delta, \mathscr{R}]$, $r^2 = \theta \in [-\theta_0/2, \theta_0/2]$ with $\theta = 0$ a Flamm paraboloid equatorial section of the spatial foil, $r^3 = \varphi \in [-\varphi_0/2, \varphi_0/2]$, and the particle path on it is $\boldsymbol{q}(t) = (x(t), y(t), z(t))$. The angular extent of the patch θ_0 is such that

$$\Omega = \Omega_r 2\sin\left(\frac{\theta_0}{2}\right)\varphi_0 \approx \Omega_r\theta_0^2 = N/n, \tag{4.3}$$

where Ω is the volume of the patch and $\Omega_r = \frac{4\pi}{3}\left[\mathscr{R}^3 - (\mathscr{R}-\delta)^3\right]$.

In natural Planck units $e^2 = 0.00729735$. Under the experimental conditions of case A of Table I we estimate that the magnitude of the geometrical potential $\sim (1/\beta)\ln(\mathscr{R}^2) \sim 10^{-24}$ is just one order of magnitude larger than the gravitational potential $Gm\mathscr{M}/\mathscr{R} \sim 10^{-25}$ that we will neglect. On the other hand, introducing the Wigner-Seitz radius $r_s = (4\pi n/3)^{-1/3}/a_0$ with $a_0 = \hbar^2/me^2$ the Bohr radius, the Copson-Linet pair potential $\sim e^2/a_0 r_s \sim 10^{-26}$ is just one order of magnitude smaller than the gravitational potential. The kinetic energy is one order of magnitude less, $\sim m(r_s/\beta)^2 \sim 10^{-27}$.

A. Effect of the neutralizing background

The charge neutrality of the jellium in the patch requires

$$\rho_b = -\frac{Ne}{\Omega} = -ne, \tag{4.4}$$

Neglecting the angular dependence of the electric field in the patch, the Poisson equation for the background potential energy ϕ_b is

$$\frac{1}{r^2}\frac{d}{dr}\left[r^2\sqrt{1-R_{\rm Sc}/r}\,E\right] = -4\pi\rho_b, \tag{4.5}$$

where $E(r) = -d\phi_b(r)/dr$ is the radial electric field. Integrating the Poisson equation from $r = R_{\rm in} = \mathscr{R} - \delta/2$ to r yields the internal electric field

$$E(r) = -\frac{4\pi\rho_b}{3}\frac{r^3 - R_{\rm in}^3}{r^2\sqrt{1-R_{\rm Sc}/r}}, \tag{4.6}$$

where we chose $E(R_{\rm in}) = 0$. Integrating $E(r)$ from $r = R_{\rm in}$ to r yields the background potential profile

$$\begin{aligned}\phi_b(r) = -\frac{8\pi e\rho_b}{3} \quad & \left\{\frac{1}{2}\left[\sqrt{r^3(r-R_{\rm Sc})} - \sqrt{R_{\rm in}^3(R_{\rm in}-R_{\rm Sc})}\right] + \right.\\ & \frac{2R_{\rm in}^3}{R_{\rm Sc}}\left[\sqrt{1-R_{\rm Sc}/R_{\rm in}} - \sqrt{1-R_{\rm Sc}/r}\right] + \\ & \frac{3R_{\rm Sc}}{4}\left[\sqrt{r(r-R_{\rm Sc})} - \sqrt{R_{\rm in}(R_{\rm in}-R_{\rm Sc})}\right] + \\ & \left.\frac{3R_{\rm Sc}^2}{4}\left[\operatorname{atanh}\sqrt{1-R_{\rm Sc}/r} - \operatorname{atanh}\sqrt{1-R_{\rm Sc}/R_{\rm in}}\right]\right\},\end{aligned} \tag{4.7}$$

Which reduces to the usual quadratic potential $\phi_b(r) \to -8\pi e\rho_b(r-R_{\rm in})^2(r+2R_{\rm in})/3r$ in the flat $R_{\rm Sc} \to 0$ limit, where we grounded the surface $r = R_{\rm in}$. The order of magnitude of the background potential for each charge is $\sim e^2 n\delta^2 \sim 10^{-26}$. For simplicity we will neglect the periodic angular images of the electrons [52]. For case A of Table I we measured $Ne_K = 1.578(7)\times 10^{-24}$ and $Ne_V = 4.9458(7)\times 10^{-23}$. So the effect of the background is to increase both the kinetic and potential energy of the plasma.

B. The black hole limit

It is interesting to study the limit of the black hole $R_{\rm Sc} \to \mathscr{R}$ or $\mathscr{M} \to \mathscr{R}/2$, keeping all other parameters fixed. By doing so we imagine a star with a mass increasing up to the point in which its Schwarzschild radius coincides with its radius. So that the star becomes a black hole. In this mathematical limit the geometrical potential diverges to $-\infty$ and, assuming that all the particles are sitting on the horizon at $r = \mathscr{R}$, the Copson pair potential (3.14) reduces to $\phi \to q_1 q_2/\mathscr{R}$, independently of their distance.

In order to get a feeling of the plasma behavior approaching the mathematical black hole limit, in our simulations we will increase the mass of the star so that, respect to the realistic white dwarf scenario, the geometrical potential will become more negative and the Copson potential will be diminished.

V. NUMERICAL RESULTS

We will choose as reference system (case A of Table I) a white dwarf with $\mathscr{R} = R_\odot 10^{-3}$, $\mathscr{M} = M_\odot$, with an atmosphere with $n = 3 \times 10^{-72}$, $T = 10^6$K. We will zoom on the patch described in the previous section with $r \in [\mathscr{R} - \delta, \mathscr{R}]$, $\theta \in [-\theta_0/2, \theta_0/2]$, and $\varphi \in [-\theta_0/2, \theta_0/2]$ with the radial width $\delta \approx \mathscr{R}\theta_0$. We will use just $N = 30$ electrons of the atmosphere and we will choose $\delta = R_\odot 10^{-20}$ and $\theta_0 = 10^{-17}$ according to (4.3).

We use the Metropolis algorithm [32, 33] to evaluate the average of Eq. (3.9).

In order to explore ergodically the positions space $\boldsymbol{r} = (r, \theta, \varphi)$ to sample the distinguishable density matrix we use the transition *displacement* move described in Appendix A of Ref. [19].

In order to sample the permutation sum of Eq. (2.12) needed for fermions we use a transition move combination of 2 Brownian *bridges* between unlike electrons as described in Appendix B of Ref. [19]. To construct a single Brownian bridge it is essential to map, project, the Schwarzschild spatial foil on a flat coordinate system. Our choice is presented in Appendix B of Ref. [19]. Perform the Gaussian bridge move in the projection flat space and then map it back to the Schwarzschild spatial foil. The Metropolis algorithm will then allow to sample the high temperature density matrix whose kinetic action is not purely Gaussian on the Schwarzschild spatial foil, due to the metric tensor appearing in $d\tilde{s}^2$.

We will work in the canonical ensemble with fixed number of particles N, electron number density $n = -\rho_b/e$, and absolute temperature $T = 1/k_B\beta$. The jellium *degeneracy parameter* is $\Theta = T/T_D$ where the degeneracy temperature $T_D = n^{2/3}\hbar^2/mk_B$ [12]. For temperatures higher than T_D, $\Theta \gg 1$, quantum effects are not very important. The *Coulomb coupling constant* is $\Gamma = \beta e^2/a_0 r_s$. At weak coupling, $\Gamma \ll 1$. The plasma becomes weakly correlated at high r_s in the classical regime, $\Theta \gg 1$, and at low r_s in the quantum regime, $\Theta \ll 1$, since the kinetic energy scales as $1/r_s^2$ and the potential energy as $1/r_s$.

In Table I we report the cases studied. We keep the electrons number density $n = 3 \times 10^{26}\text{cm}^{-3}$, the number of electrons $N = 30$, and the patch geometry fixed and we vary the temperature. As we can see from the values of r_s, Γ, and Θ for cases A, B, C the atmosphere is expected to be in the quantum regime and weakly correlated. Case M is like case A but with $\mathscr{M} = 0$ so that the geometrical effect of gravity is canceled. Case BH is like case A but with $\mathscr{M} = 10^{40}$ so that the Schwarzschild radius comes closer to the plasma by ≈ 110 solar masses.

Apart from thermodynamic properties like the *kinetic energy* per particle, const $- e_K > 0$, the *Coulomb potential energy* per particle, e_V, [13] and the *geometrical potential energy* per particle, e_W, we will also measure structural properties like the *radial distribution function* (RDF), $g(r) = \langle \mathscr{O} \rangle$. For it we used the following histogram estimator,

$$O(R; r, a) = \sum_{m \neq n} \frac{1_{]r-\Delta/2, r+\Delta/2]}(d_{mn})}{N n_{id}(r)}, \tag{5.1}$$

where Δ is the histogram bin, $1_{]u,v]}(x) = 1$ if $x \in]u, v]$ and 0 otherwise, d_{mn} is the Euclidean distance between 2 electrons m, n [14]

$$d_{mn} = d(\boldsymbol{r}_m, \boldsymbol{r}_n) = \sqrt{(\boldsymbol{q}_n - \boldsymbol{q}_m) \cdot (\boldsymbol{q}_n - \boldsymbol{q}_m)}, \tag{5.2}$$

and

$$n_{id}(r) = 4\pi n \left[(r + \Delta/2)^3 - (r - \Delta/2)^3 \right] /3 \ , \tag{5.3}$$

is the average number of particles on the spherical shell $]r - \Delta/2, r + \Delta/2]$ for the ideal gas of density n. We have that $n^2 g(r)$ gives the probability, that sitting on a particle at $\boldsymbol{r}$, one finds another particle at $\boldsymbol{r}'$ with $r = d(\boldsymbol{r}, \boldsymbol{r}')$.

Fermions properties cannot be calculated exactly with path integral Monte Carlo because of the *fermions sign problem* [34, 53]. We then have to resort to an approximate calculation. The one we chose was the Restricted Path Integral (RPIMC) approximation [24, 34, 53, 54] with a "free fermions restriction". The trial density matrix used in the *restriction* is chosen as the one reducing to the ideal density matrix in the limit of $t \ll 1$ and is given by the following explicit analytic expression,

$$\rho_0(R_k, R_l; t) \propto \det \left|\left| e^{-\frac{d^2(\boldsymbol{r}_{i,k}, \boldsymbol{r}_{j,l})}{4\lambda t}} \right|\right| . \tag{5.4}$$

---

[12] This is the temperature at which the size of a single electron path, in absence of interaction, i.e. the thermal wavelength $(2\lambda\beta)^{1/2}$, equals the separation between single particle paths, i.e. roughly $n^{-1/3}$. Below this temperature it is possible for single particle paths to link up exchanging their end points.

[13] The estimators for these observables are carefully described in Ref. [11].

[14] Here it is important to expand $\cos\gamma_{mn} - 1$ of Eq. (3.15) at least to second order in θ_i, φ_i for $i = n, m$ in order to have the correct behavior of the RDF at small distances.

TABLE I. Cases treated in our simulations: $\mathscr{R}$ the white dwarf radius, δ the patch radial width, $\mathscr{M}$ the white dwarf mass, N the number of particles, r_s the Wigner-Seitz radius, β the inverse temperature. The adimensional quantities Γ and Θ were introduced in the main text. The results for the thermodynamic quantities, $e_K = \langle K\rangle/N$ from the thermodynamic estimator $K(R,R';\tau) = \tilde{g}_{\mu\nu}(R)(R-R')^\mu(R-R')^\nu/4\lambda\tau^2$ as explained in Ref. [11], $e_V = \langle V\rangle/N$ the Coulomb potential energy per particle, and $e_W = \langle W\rangle/N$ the geometrical potential energy per particle, are given for the simulation without the sum over the permutations in Eq. (2.12) and with the permutations sum in the bottom table. In the RPIMC case we also report the average number of two particles exchanges $< N$. We neglected the presence of the neutralizing background of Section IV A. We chose natural Planck units with $c = G = \hbar = k_B = 1$. The simulation lasted not less than 10^5 Monte Carlo steps where one step is made of a displace move of all the beads of a single particle path as described in Appendix A of Ref. [19] and a bridge move as described in Appendix B of Ref. [19].

case	M	N	$\mathscr{R}$	δ	$\theta_0 = \varphi_0$	$\mathscr{M}$	β	$a_0 r_s$	r_s	Γ	Θ
A	30	30	$R_\odot 10^{-3}$	$R_\odot 10^{-20}$	10^{-17}	$M_\odot$	1.4×10^{26}	2×10^{23}	0.061	5.17	0.03
B	300	30	$R_\odot 10^{-3}$	$R_\odot 10^{-20}$	10^{-17}	$M_\odot$	1.4×10^{27}	2×10^{23}	0.061	51.7	0.003
C	3	30	$R_\odot 10^{-3}$	$R_\odot 10^{-20}$	10^{-17}	$M_\odot$	1.4×10^{25}	2×10^{23}	0.061	0.517	0.3
M	30	30	$R_\odot 10^{-3}$	$R_\odot 10^{-20}$	10^{-17}	0	1.4×10^{26}	2×10^{23}	0.061	5.17	0.03
BH	30	30	$R_\odot 10^{-3}$	$R_\odot 10^{-20}$	10^{-17}	$109.4M_\odot$	1.4×10^{26}	2×10^{23}	0.061	5.17	0.03

	PIMC no permutations			RPIMC with permutations			
case	$Ne_K(\times10^{-24})$	$Ne_V(\times10^{-23})$	$-Ne_W(\times10^{-21})$	# swaps	$Ne_K(\times10^{-24})$	$Ne_V(\times10^{-23})$	$-Ne_W(\times10^{-21})$
A	1.627(2)	4.6549(1)	1.178895	25.6(2)	1.637(3)	4.6550(2)	1.178895
B	1.636(2)	4.6546(2)	1.178895	20.3(6)	1.637(4)	4.6548(3)	1.178895
C	1.605(2)	4.6548(1)	1.178895	26.01(3)	1.643(3)	4.6549(2)	1.178895
M	–	–	–	26.0(1)	1.627(2)	4.6548(2)	1.178881
BH	–	–	–	26.1(1)	2.104(4)	4.2502(2)	1.180852

Note that here we purposely chose the Euclidean distance (5.2). We did this just for the sake of simplicity. In any case both the Euclidean and the geodesic distance reduce to $ds^2(\boldsymbol{r}_{i,k},\boldsymbol{r}_{j,l}) = g_{\alpha\beta}(\boldsymbol{r}_i)(\boldsymbol{r}_{i,k}-\boldsymbol{r}_{j,l})^\alpha(\boldsymbol{r}_{i,k}-\boldsymbol{r}_{j,l})^\beta$ in the $t = \tau|k-l| \ll 1$ limit. The implementation of the RPIMC on a curved space has already been described in section IV B of Ref. [19]. The permutation sampling necessary to compute the sum in Eq. (2.12) is carried out through the composition of two Brownian bridges and a swap of two identical particles (we explicitly neglected 3 particles permutation cycles). The realization of a Brownian bridge on the curved Schwarzschild space used a mapping onto a flat space as explained in appendix B of Ref. [19] with the only care of distinguishing between a radial standard deviation $\sigma_r = \sqrt{2\lambda\tau}$ and an angular one $\sigma_a = \sigma_r/\mathscr{R}$ for the Gaussian in the flat projected space (r,θ,φ).

We start the simulation with random beads of each electron at each timeslice within the subatomic patch. In case A of Table I we simulate the white dwarf at different temperatures: $T = 10^6$K, in case B $T = 10^5$K, and in case C $T = 10^7$K. Case M is like case A but in absence of with $\mathscr{M} \to 0$. And case BH is like case A but with a larger mass of the star approaching the black hole limit described in Section IV B. In all cases we keep a fixed timestep $\tau = \beta/M = 4.7\times10^{24}$ in Planck units. For each case we use either the PIMC treating the electrons as Boltzmannons, neglecting the permutations sum in Eq. (2.12) and the RPIMC which correctly but approximately treats the electrons as Fermions.

From the table we see how the potential, Coulomb or geometrical, does not change appreciably between cases A,B,C. On the other hand, the kinetic energy increases with temperature in the simulations without the permutations and has the opposite behavior when RPIMC is used. Quantum statistics affects Ne_K by $\sim 1\%$. The relative difference of the geometrical potential of case A and M is $\sim 10^{-5}$ while the kinetic energy relative difference is already $\sim 10^{-2}$. Approaching the black hole limit the geometrical potential becomes more negative, the Copson potential is lowered, and the kinetic energy diminishes. This is shown by comparing cases A and BH of the Table.

In Fig. 2 we show the RDF for the three cases A,B,C of Table I without the electrons permutations. The peak of the RDF is at a distance $\Delta r \approx a_o r_s/4 \sim 10^{23}\times10^{-33}\text{cm} \sim 10^{-2}$Å. This means that two electrons are likely to be found closer than the Wigner-Seitz radius. From the figure we see how $g(r\to0)\to0$ in agreement with the divergence of the Coulomb potential when the two electrons coincide. The patch geometry accommodates just the

first oscillation of the RDF which otherwise would tend to $g(r \to \infty) \to 1$. The extremely high peak can be explained as due to the geometry of the patch. Compare with the RDF of Euclidean jellium in a periodic cubic box [26]. We see how the change in temperature does not produce an appreciable change in the RDF. The same can be said for the effect of the Fermi statistics or the geometrical effect of gravity.

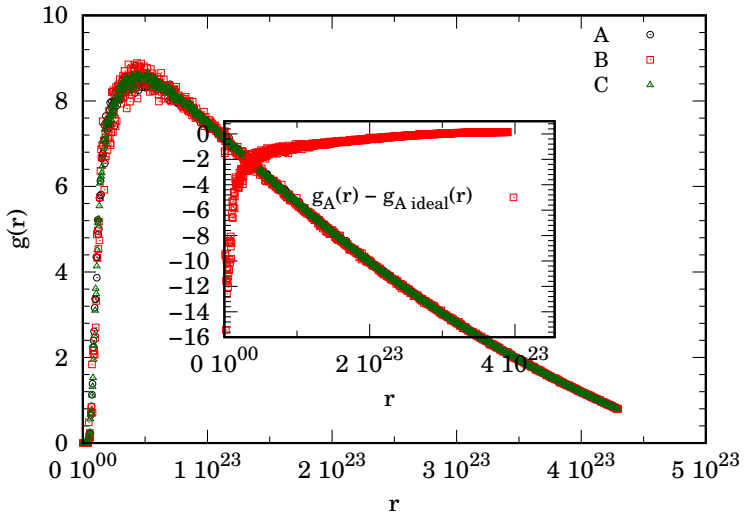


FIG. 2. The RDF for cases A,B,C of Table I without permutations. We explicitly verified that taking into account the permutations among the electrons does not change appreciably the RDF. The RDFs of cases M and BH are also not appreciably different from the one of case A shown here. The radial distance r is in Planck units 1.61623×10^{-33}cm. The radial length of the patch is $\delta = 4.3 \times 10^{23}$. In the inset we show the difference between the RDF of case A and the RDF of case A without the Copson pair potential between the electrons.

In Fig. 3 we show a snapshot of the electrons paths in the coordinates (r, θ, φ) in the plasma for the patch of case A with RPIMC of Table I at thermal equilibrium.

VI. CONCLUSIONS

Still largely unknown is the process of cooling of a white dwarf. We think that the dead star still possesses some activity in its thin radiating atmospheric layer. Which is the source of the luminosity that we are able to measure. It is therefore important to be able to understand the properties, thermodynamic and structural, of the plasma that forms the atmosphere.

In this work we simulated a subatomic patch of this layer. We modeled the plasma as a jellium where we initially neglect the effect of the uniform neutralizing background. For the Coulomb pair potential between the electrons we adopted the Copson solution for particles living in a spatial section of the Schwarzschild metric. We modeled the patch of the dimensions of Å/20 using periodic boundary conditions on the spherical angles and wall boundary conditions on the radial coordinate. The expected experimental conditions of the plasma suggest that it will be weakly interacting and the quantum statistics will play a non negligible role. Therefore we used the path integral Monte Carlo method to estimate the quantum effects. We found that quantum statistics affects the third significant figure of the kinetic energy. We then used the Schwarzschild solution of Einstein field equations to estimate the *geometrical* effect of gravity. These also affect the third significant figure of the kinetic energy. Our measure of the radial distribution function does not feel appreciably any of these effects, temperature, quantum statistics, or *geometrical* gravity.

We then imagined a situation where we increase the mass of the star keeping all other parameters constant so to let the event horizon come closer to the patch and we noticed a diminution of both the kinetic and the potential energy of the plasma. Both the geometrical and the Coulomb potential energies diminish.

Comparing with the phase diagram of jellium in Euclidean space we see how in our case A we are on the lower left corner of figure 1 of Ref. [26] so that in order to see a crystallization we should at the same time wait for the star to cool down and observe the outer more rarefied part of the atmosphere.

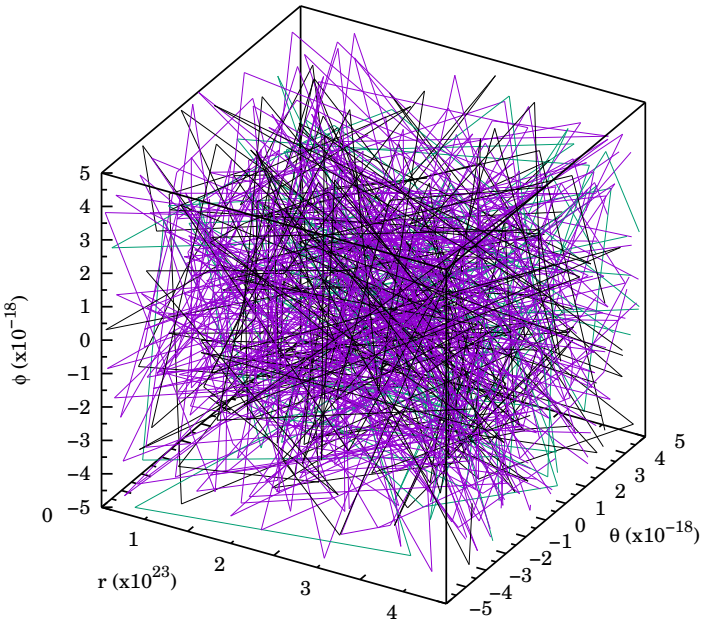


FIG. 3. Snapshot of the Coulomb plasma of case A of Table I with permutations. The radial distance r is in Planck units 1.61623×10^{-33}cm. The paths of the 30 electrons are painted with different colors for different permutations cycles.

AUTHOR DECLARATIONS

Conflicts of interest

None declared.

Data availability

The data that support the findings of this study are available from the corresponding author upon reasonable request.

Funding

None declared.

[1] S. L. Shapiro and S. A. Teukolsky, *Black Holes, White Dwarfs, and Neutron Stars. The Physics of Compact Objects* (John Wiley & Sons Inc, New York, 1983).
[2] S. Chandrasekhar and E. A. Milne, The Highly Collapsed Configurations of a Stellar Mass, Monthly Notices of the Royal Astronomical Society **91**, 456 (1931).
[3] S. Chandrasekhar, The Density of White Dwarf Stars, Phil. Mag. **11**, 592 (1931).
[4] S. Chandrasekhar, The Maximum Mass of Ideal White Dwarfs, Astrophys. J. **74**, 81 (1931).
[5] R. Fantoni, White-dwarf equation of state and structure: the effect of temperature, J. Stat. Mech. , 113101 (2017).
[6] R. C. Tolman, Static Solutions of Einstein's Field Equations for Spheres of Fluid, Phys. Rev. **55**, 364 (1939).

[7] J. R. Oppenheimer and G. M. Volkoff, On Massive Neutron Cores, Phys. Rev. **55**, 374 (1939).
[8] N. H. March and M. P. Tosi, *Coulomb Liquids* (Academic Press Inc Ltd, London, 1984).
[9] M. Gell-Mann and K. A. Bruckner, Correlation Energy of an Electron Gas at High Density, Phys. Rev. **106**, 364 (1957).
[10] K. S. Singwi, M. P. Tosi, R. H. Land, and A. Sjölander, Electron Correlations at Metallic Densities, Phys. Rev. **176**, 589 (1968).
[11] D. M. Ceperley, Path integrals in the theory of condensed Helium, Rev. Mod. Phys. **67**, 279 (1995).
[12] D. M. Ceperley and B. J. Alder, Ground State of the Electron Gas by a Stochastic Method, Phys. Rev. Lett. **45**, 566 (1980).
[13] R. Fantoni, Radial distribution function in a diffusion Monte Carlo simulation of a Fermion fluid between the ideal gas and the Jellium model, Eur. Phys. J. B **86**, 286 (2013).
[14] R. Fantoni, Many Body in General Relativity: A thermal equivalence principle, Quantum Rep. **8**, 42 (2026).
[15] R. Fantoni, Statistical Gravity through Affine Quantization, Quantum Rep. **6**, 706 (2024).
[16] R. Fantoni, Statistical Gravity and entropy of spacetime, Stats **8**, 23 (2025).
[17] R. Fantoni, Statistical Gravity, ADM splitting, and Affine Quantization, Gravitation and Cosmology **31**, 568 (2025).
[18] R. Fantoni, *Unifying Classical and Quantum Physics - How classical and quantum physics can pass smoothly back and forth* (Springer, New York, 2025).
[19] R. Fantoni, Path Integral Monte Carlo on a Sphere, Phys. Rev. B **114**, 185409 (2026).
[20] R. Arnowitt, S. Deser, and C. Misner, The Dynamics of General Relativity, In: Witten, L., Ed., Gravitation: An Introduction to Current Research, Wiley & Sons, New York, 227 (1962), arXiv: gr-qc/0405109.
[21] R. Fantoni, Formalism for the Matter Density Matrix in an ADM $3+1$ foliation of spacetime, Phys. Rev. Lett. (in preparation) (2026), `https://rfantoni.github.io/personal-page/publications/pcdms.pdf`.
[22] R. C. Tolman, On the Weight of Heat and Thermal Equilibrium in General Relativity, Phys. Rev. **35**, 904 (1930).
[23] R. C. Tolman and P. Ehrenfest, Temperature Equilibrium in a Static Gravitational Field, Phys. Rev. **36**, 1791 (1930).
[24] R. Fantoni, One-component fermion plasma on a sphere at finite temperature, Int. J. Mod. Phys. C **29**, 1850064 (2018).
[25] R. Fantoni, One-component fermion plasma on a sphere at finite temperature. The anisotropy in the paths conformations, J. Stat. Mech. , 083103 (2023).
[26] E. W. Brown, B. K. Clark, J. L. DuBois, and D. M. Ceperley, Path-Integral Monte Carlo Simulation of the Warm Dense Homogeneous Electron Gas, Phys. Rev. Lett. **110**, 146405 (2013).
[27] F. Becattini, Covariant Statistical Mechanics and the Stress-Energy Tensor, Phys. Rev. Lett. **108**, 244502 (2012).
[28] H. Andréasson, The Einstein-Vlasov System/Kinetic Theory, Living Reviews in Relativity **14**, 10.12942/lrr-2011-4 (2011).
[29] F. R. S. Paul Adrien Maurice Dirac, Quantised singularities in the electromagnetic field, Proc. R. Soc. A **133**, 60 (1931).
[30] L. S. Schulman, *Techniques and Applications of Path Integration* (John Wiley & Sons, Technion, Haifa, Israel, 1981) chapter 24.
[31] B. S. DeWitt, Dynamical Theory in Curved Spaces. I. A Review of the Classical and Quantum Action Principles, Rev. Mod. Phys. **29**, 377 (1957).
[32] N. Metropolis, A. W. Rosenbluth, M. N. Rosenbluth, A. M. Teller, and E. Teller, Equation of state calculations by fast computing machines, J. Chem. Phys. **1087**, 21 (1953).
[33] M. H. Kalos and P. A. Whitlock, *Monte Carlo Methods* (John Wiley & Sons Inc., New York, 1986).
[34] D. M. Ceperley, Path integral Monte Carlo methods for fermions, in *Monte Carlo and Molecular Dynamics of Condensed Matter Systems*, edited by K. Binder and G. Ciccotti (Editrice Compositori, Bologna, Italy, 1996).
[35] R. Fantoni, The density of a fluid on a curved surface, J. Stat. Mech. , P10024 (2012).
[36] F. Bastianelli and O. Corradini, On the simplified path integral on spheres, Eur. Phys. J. C **77**, 731 (2017).
[37] A. Lenard, Exact Statistical Mechanics of a One Dimensional System with Coulomb Forces, J. Math. Phys. **2**, 682 (1961).
[38] S. F. Edards and A. Lenard, Exact Statistical Mechanics of a One Dimensional System with Coulomb Forces. II. The Method of Functional Integration, J. Math. Phys. **3**, 778 (1961).
[39] A. M. Salzberg and S. Prager, Equation of State for a Two-Dimensional Electrolyte, J. Chem. Phys. **38**, 2587 (1963).
[40] B. Jancovici, Exact Results for the Two-Dimensional One-Component Plasma, Phys. Rev. Lett. **46**, 386 (1981).
[41] P. Choquard, Helv. Phys. Acta **54**, 332 (1981).
[42] J. M. Caillol, Exact results for a two-dimensional one-component plasma on a sphere, J. Phys. (France) - Lett. **42**, L (1981).
[43] R. Fantoni, B. Jancovici, and G. Téllez, Pressures for a One-Component Plasma on a Pseudosphere, J. Stat. Phys. **112**, 27 (2003).
[44] R. Fantoni and G. Téllez, Two dimensional one-component plasma on a Flamm's paraboloid, J. Stat. Phys. **133**, 449 (2008).
[45] R. Fantoni, Two component plasma in a Flamm's paraboloid, J. Stat. Mech. , P04015 (2012).
[46] J. R. Klauder, Quantization of Constrained Systems, in *Methods of Quantization*, Lecture Notes in Physics, Vol. 572, edited by H. Latal and W. Schweiger (2001) p. 143.
[47] J. H. V. Vleck, The Correspondence Principle in the Statistical Interpretation of Quantum Mechanics, Proc Natl Acad Sci U S A **14**, 178 (1928).
[48] H. F. Trotter, On the Product of Semi-Groups of Operators, Proc. Am. Math. Soc. **10**, 545 (1959).
[49] E. T. Copson, On electrostatics in a gravitational field, Proceedings of the Royal Society of London **118**, 184 (1928).
[50] B. Linet, Electrostatics and magnetostatics in the Schwarzschild metric, Journal of Physics A: Mathematical and General **9**, 1081 (1976).

[51] B. Linet, Electrostatic self-force and material sources of the gravitational field, General Relativity and Gravitation **18**, 731 (1986).
[52] V. Natoli and D. M. Ceperley, An Optimized Method for Treating Long-Range Potentials, Comput. Phys. **117**, 171 (1995).
[53] D. M. Ceperley, Fermion Nodes, J. Stat. Phys. **63**, 1237 (1991).
[54] R. Fantoni, Jellium at finite temperature, Mol. Phys. **120**, 4 (2021).

Supplementary Files

This is a list of supplementary files associated with this preprint. Click to download.

- wdpimcs.pdf